Arctic sediment routing during the Triassic - sinking the Arctic Atlantis

Albina Gilmullina, Tore Grane Klausen, Anthony George Doré, Hallgeir Sirevaag,

Anna Suslova, Christian Haug Eide

Arctic sediment routing during the Triassic - sinking the Arctic Atlantis

Albina Gilmullina[1*], Tore Grane Klausen[2], Anthony George Doré[3], Hallgeir Sirevaag[1] Anna Suslova[4], Christian Haug Eide[1]

[1] Department of Earth Science, University of Bergen, Allégaten 41, 5007 Bergen, Norway,

[2]M Vest Energy AS, Edvard Griegs vei 3, 5059 Bergen, Norway

[3] Energy & Geoscience Institute (EGI), University of Utah, 423 Wakara Way, Suite 300 Salt Lake City, Utah 84108

[4]Petroleum Department, Lomonosov Moscow State University, 1 Leninskiye Gory, 119991 Moscow, Russia

ORCID ID: Albina Gilmullina 0000-0001-6187-9029; Tore Grane Klausen 0000-0003-2524-512X; Hallgeir Sirevaag 0000-0001-8195-3505; Christian Haug Eide 0000-0003-4949-9917

**Corresponding author (e-mail: albina.gilmullina@uib.no)*

Abstract

Opening of the Arctic Ocean has been the subject of much debate, and the placement of terranes in Early Mesozoic remains a crucial part of this important discussion. Several continental terranes complicate the paleogeographic reconstruction. One such terrane is Crockerland, which has been inferred to explain sediment distribution in the Arctic throughout the Mesozoic. However, the Triassic successions throughout the Arctic basins bear many similarities, and a common sedimentary source could offer a simpler explanation with fewer implications for the basin configuration in the Arctic. The study's goal is to test the hypothesis of long-distance sediment transport from a common source to all Arctic basins in the Triassic,

and to demonstrate how estimates of sediment routing distances can improve pre-breakup plate tectonic reconstructions.

Results confirm that (1) the Arctic basins were closely connected prior to breakup in the Mesozoic, (2) based on regional facies distribution, sediment budgets, sediment modelling and detrital zircon age spectra, the Crockerland terrane is unlikely to have existed, (3) the reconstructed Arctic sediment routing system can help to constrain plate tectonic models, (4) and statistical estimate of sediment transport is a novel and potentially important tool for improving plate tectonic and paleogeographic reconstructions.

Supplementary material

DR1 LA-ICPMS zircon data

Placement of micro-continents in the Arctic before the breakup in the Early Cretaceous is a controversial issue and many different reconstructions have been proposed (e.g., Shephard et al., 2013; Miller et al., 2013; 2018; Sømme et al., 2018; Nikishin et al., 2019, Fig. 1). Understanding pre-breakup sediment transport across sedimentary basins in the Arctic could help constrain locations of microcontinents and improve plate-tectonic models, because sediment with known transport routes may serve as “piercing points” in previously adjacent basins (e.g. Richardson et al., 2017). Sediment transport distance and distribution also serves as a holistic sense-check, whereby the basin configuration is considered with a source-to-sink perspective with multi-disciplinary implications for regional tectonics. Enormous sediment volumes were produced in, and prograded from, the Urals and West Siberia in the Carnian and Norian (Late Triassic) across the Greater Barents Sea Basin and Svalbard (GBSB, Klausen et al., 2019; Gilmullina et al., 2021a; Fig. 2). The mapping and budgeting of these deposits offer improved understanding of plate tectonic process and relative positioning of terrains in the Arctic.

A micro-continent named Crockerland has previously been inferred between GBSB and the Sverdrup Basin (Fig. 1) based on lithologic- and facies patterns in these two areas (Mørk et al., 1989; Embry, 1993). Recent analysis show the Triassic sediments in GBSB including the Late Triassic in Svalbard are characterized by 1) a large proportion of mudstone, 2) fine- to very fine-grained sandstones (Fig. 3), and 3) a detrital zircon spectrum with a dominant Paleozoic peak and a small number of "young" zircons close to depositional age (time span between c. 210 and 245 Ma, Bue and Andresen, 2014; Klausen et al., 2015; Fleming et al., 2016; Flowerdew et al., 2019; Figs. 4, 5), which were supplied from sediment sources in the Urals and West Siberia, rather than Crockerland in the north (Fig 1A). These sediment properties are similar to those observed in the Late Triassic in the Sverdrup Basin (Embry, 1997; Omma et al., 2011; Anfinson et al., 2016). Furthermore, seismic data (Fig.2, Gilmullina et al., 2021a) and sediment volume modelling (Fig. 6) show bypass of large amounts of sediments from the GBSB into adjacent basins (Gilmullina et al., 2021b). This raises the possibility that sediments previously believed to have originated from Crockerland, in fact originated from the Urals and West Siberia and were transported a long distance across mainly subsiding basins.

An understanding of how far the sediments sourced from the Urals and West Siberia could have reached into these adjacent basins is currently lacking. Estimation of the sediment volumes bypassed off the GBSB and size of the potentially receiving basins gives necessary inputs for calculation the length of the system beyond the GBSB.

The goals of this study are fourfold: 1) to present a novel method to determine sediment routing system, developed based on sediment budget calculations and investigation of provenance data, 2) to develop a model that explains Triassic sediment transport in the Arctic, 3) to evaluate whether Crockerland is a necessary concept for the Upper Triassic of the Arctic, and 4) discuss how these results compare with existing plate-tectonic reconstructions for the Arctic,

Triassic arctic stratigraphy

In the Triassic the Arctic comprised five main sedimentary basins, including: GBSB, Sverdrup Basin, West Chukotka Basin, Arctic Alaska and East Siberian Sea Basin (Fig. 1). Our review of the stratigraphic development in these basins (based on Glørstad-Clark et al., 2010; Klausen et al., 2015; Gilmullina et al. 2021; Rossi et al., 2019; Embry 1997; Tuchkova et al., 2009; Moore et al., 2002; Zakharov et al., 2010) shows that they share a common pattern in the sedimentation rates, with large amounts of sediments supplied in the Early Triassic, small amounts in the Middle Triassic, and large amounts in the Late Triassic. However, local variations are also evident:

The GBSB filled with up to 4.5 km of sediments, supplied through a linked clinoform/mud-belt-delta-coastal plain system from the Urals and West Siberia - Uralo-Siberian source (Klausen et al., 2015; Gilmullina et al., 2021a; Figs. 3b, 7). These are represented by a large proportion of mudstone, mineralogically immature and fine-grained sandstones (Bergan and Knarud, 1993), late Paleozoic to Triassic detrital zircons (Bue and Andresen, 2013; Fleming et al., 2016; Klausen et al., in press.) and large sediment volumes (Gilmullina et al., 2021b). Three hundred meters the Late Triassic fluvial deposits are found in outcrops on Svalbard and Hopen Island (Klausen and Mørk, 2014; Lord et al., 2015; Riis et al. 2008) and confirm a northwesterly sediment transport direction (Klausen and Mørk, 2014; Haile et al., 2018), indicating that the late Carnian delta system (C3 and C4 units) reached and prograded over the most northwestern part of the GBSB. In the GBSB the early Norian (N1 unit) delta system “back-stepped” (Klausen at al., 2015) and prograded again over Svalbard and the western margin of the GBSB in the late Norian (N2 unit) (Fig. 3b, Klausen et al., 2015).

The Uralo-Siberian source had a continental-scale drainage system, able to supply sediment volumes comparable to present-day continental margin volumes, which overspilled into adjacent Arctic basins (Gilmullina et al., 2021b). Towards the basin margins to Fennoscandia and Greenland, smaller amounts of mature sediments with older detrital zircon age spectra also occur (Bue & Andresen, 2014; Eide et al., 2018; Fig. 3b). Organic rich mudstones of the Steinkobbe and Botneheia formations were deposited in areas so distal they did not receive coarser clastic sediments from the prograding deltas and were particularly widespread in the Middle Triassic when sediment supply to the basin was smaller (e.g., Krajewski and Weitschat, 2015; Krajewski, 2008; Fig. 3b).

The Sverdrup Basin was infilled by deltas, mainly derived from eroded Devonian strata in Arctic Canada and Greenland (Bjorne Fm) (Fig. 3a), during the Early Triassic (Anfinson et al., 2016). The Middle Triassic was dominated by dark bituminous shales about 60 m thick (Murray Harbour Fm) (Embry 1997), similar to time-equivalent strata in Svalbard and distal parts of the GBSB (Steinkobbe and Botneheia formations). In the Late Triassic, large amounts of mudstone-rich sediments with very fine- to fine-grained sediments up to 1400 m thick (Hoyle Bay and Pat Bay and Romulus members, Heiberg Fm) were derived from the north, and prograded as shallow marine to deltaic environments southward across much of the basin (Embry, 1997; Fig. 3a). The traditional view is that these northerly-derived sediments were supplied from a northern landmass that has been named Crockerland (Fig. 1; Embry, 1993). The detrital zircon spectra from these sediments in the Sverdrup Basin were discovered to show the typical

Uralo-Siberian source-signature, as also seen in the GBSB (Figs. 4a-c, 5), leading to a slight modification of this hypothesis by its proponents whereby these sediments were transported from the Urals and West Siberia to the Sverdrup Basin through a low-lying but emergent Crockerland (Anfinson et al., 2016; Embry and Beauchamp, 2019; Galloway et al., 2021; Colpron and Nelson, 2011). Below, we will make the case that these sediments were not supplied from Crockerland at all but are rather the result of overspill of sediments derived from the Uralo-Siberian source through Svalbard and the northern part of GBSB.

Sediments in the West Chukotka Basin were supplied by large delta systems, but the Lower-Middle Triassic deposits were dominated by distal turbiditic, deep-marine continental slope-equivalents to these deltas (Tuchkova et al., 2009). During the Carnian, the West Chukotka Basin was dominated by shelf to base-of-slope environments and contains a thick (up to 2 km) package of turbidities, whereas the Norian interval mostly represents a shallow shelf environment, with sediments up to 1 km thick (Tuchkova et al., 2009; Fig. 3c).

During the Early Triassic, the eastern and central parts of Arctic Alaska were dominated by a fan-delta (Ivishak Fm) sourced locally from Laurentia and prograded basinwards to the deep shelf from the north (Houseknecht, 2019). The Middle-Upper Triassic is represented by siliciclastic, carbonate and phosphatic deposits of Shublik Fm and a clastic wedge in its upper part. The latter, the Sag River Sandstone, represents a fine-grained marine shelf sourced from Laurentia (or the northeast in modern coordinates (Mozley and Hoernle, 1990). Throughout the Triassic, western Alaska faced the paleo-Pacific Ocean and was dominated by an outer shelf environment represented by phosphatic, black shale, chert, silicified limestone of the Otuk Fm (Tye et al., 1999; Moore et al., 2002; Houseknecht, 2019, Fig. 3d), characteristic of a relatively sediment-starved submarine basin. The Karen Creek siltstone member in the upper part of the Otuk Fm is, in contrast, represented by very fine to fine-grained sandstone deposited as turbidites (Moore et al., 2002; Whidden et al., 2018). The Karen Creek siltstone member was supplied from the east, possibly from Chukotka, and it is time-equivalent to the Sag River Sandstone (Fig.3d).

Triassic deposits on the New Siberian Islands are characterized by thin (up to 600 m) shale-dominated deep-water deposits with carbonates, phosphorite and siderite concretions (Egorov et al., 1987; Zakharov et al., 2010).

Thus, as shown above, the Arctic basins show two general patterns: Firstly, a pattern where the sediment supply is high in the Early Triassic, low and dominated in distal areas by marine productivity during the Middle Triassic, and high again during the late Triassic. Secondly, sediments shed from local sources become gradually replaced by mudstone-rich sediment with a Late Paleozoic and Triassic detrital zircon age peak. This would indicate that these now separated basins were linked prior to breakup, and that sediments were supplied to these basins across significant distances. Whether the sediment budget and catchment characteristics are sufficient to provide enough material to prograde these distances is a key question. Sediment budget for individual time series and their provenance character can tell us whether the progradation length is reasonable and if the sediment source is similar in these areas, and this will be addressed below.

Methods

Dataset

Here we used the database of sediment volumes, stratigraphic seismic interpretations and sediment transport directions based on analysis of 3238 seismic 2D lines, 20 3D seismic datasets, 257 wells and 39 biostratigraphic datings; detrital zircon database consisting of 2 new and 16 published samples; sediment volumes and sediment supply rates in GBSB of all stratigraphic units on Fig. 3b.

Sediment volume estimations

Gilmullina et al., (2021b) shows sediment volumes supplied to the basin per year using two different methods: 1) based on *observed* volumes calculated from seismic dataset, and 2) *modelled* volumes from the BQART approach involving Monte-Carlo Simulation (MCS). Observed volumes calculations are based on i) estimation of the time-thickness of each stratigraphic time unit, determined by interpreting the available dataset described above, ii) depth-conversion of top and bottom surfaces of each time unit, iii) calculation of the mass of each unit by multiplying thickness maps with density maps, created based on density logs from available wells, iv) division of mass of each time unit by duration determined by biostratigraphic data.

Modelled volumes are based on the empirical BQART model created by Syvitski and Milliman (2007). The model depends on input variables and shows the sediment load from the catchments supplying sediments to the sink that could be described by the following equation:

$$Q_s = \omega L Q_w^{0.31} A^{0.5} R T \quad (1)$$

where Q_s is sediment discharge (10^6 t/yr), ω is an empirical constant (ω = 0.0006), L is a variable for bedrock erodibility (with extremes of 0.5 to 3 for hard metamorphic/plutonic bedrock lithologies and erodible loess lithology, respectively), Q_w is annual water discharge (km^3/yr), A is catchment area (km^2), R is maximum catchment relief (km), and T is the long-term basin-averaged temperature (°C). Gilmullina et al. (2021b) used Monte Carlo simulations (MCS) to model sediment supply based on realistic catchment parameters described above. Each input parameter was assigned to a normal distribution within limits, and the MCS performed 5000 realizations per stratigraphic unit. The methods are explained in detail in a previous paper, Gilmullina et al. (2021b).

Detrital zircon age analysis

Here, we present new detrital zircon U/Pb ages from two samples: one outcrop sample from the Induan Vardebukta Fm. in the Festningen section on Svalbard, and one drill core sample from the Induan Havert Fm. on the Finnmark Platform (well 7128/9-U-1 (83.40 m)). The drill core sample was made available by the Norwegian Petroleum Directorate (NPD).

The samples were crushed with a disc-mill, before the zircons were concentrated, using panning and density separation techniques. Instead of hand-picking, the zircons were extracted for mounting by pipetting of ethanol to limit bias during picking. The zircons were then embedded in epoxy, ground to c. half the grain thickness and polished. The grain mounts were further photographed with backscatter (BS) and cathodoluminescence (CL) detectors, using a Zeiss Supra 55VP Scanning Electron Microscope, prior to Laser Ablation Inductively Coupled Plasma Mass Spectrometer (LA-ICP-MS) analyses at Bergen Geoanalytical Facility, University of Bergen.

For each sample, 331 – 349 zircons were analyzed by a Nu AttoM high-resolution ICP-MS, coupled to a 193 nm ArF excimer laser (Resonetics RESOlution M-50 LR). The laser was fired at a repetition rate of 5 Hz and with an energy of 90 mJ, using a spot size of 26 µm. Typical acquisitions consisted of 15 s measurement of blank, followed by 30 s of measurement of U, Th, and Pb signals from the ablated zircon. The data were acquired in time resolved–peak jumping–pulse counting mode with 1 point measured per peak for masses ^{204}Pb + Hg, ^{206}Pb, ^{207}Pb, ^{208}Pb, ^{232}Th, ^{235}U, and ^{238}U. The raw data were preprocessed using a purpose-made Excel macro due to a nonlinear transition between the counting and attenuated (=analog) acquisition modes of the ICP instruments. As a result, the intensities of ^{238}U were left unchanged if measured in a counting mode and recalculated from ^{235}U intensities if the ^{238}U was acquired in an attenuated mode. The data reduction (correction for gas blank, laser-induced elemental fractionation of Pb and U, and instrument mass bias) was carried out off-line using the Iolite data reduction package (v. 3.0), with VizualAge utility (Petrus & Kamber, 2012). Details of the data reduction methodology can be found in Paton et al., 2010. For the data presented here, blank intensities and instrumental bias were interpolated using an automatic spline function, while down-hole interelement fractionation was corrected using an exponential function. No common Pb correction was applied to the data, but the low concentrations of common Pb were controlled by observing the $^{206}Pb/^{204}Pb$ ratio during measurements. Residual elemental fractionation and instrumental mass bias were corrected by normalization to the natural zircon reference material 91500 (1065 Ma: Wiedenbeck et al., 1995). Zircon reference materials GJ-1 (609 Ma: Jackson et al., 2004) and Plešovice (337 Ma: Sláma et al., 2008) were periodically analyzed during the measurement for quality control. The GJ-1 and Plešovice standards provided ages of 599.2 ± 0.4 Ma and 345.2 ± 0.3 Ma, respectively, when calibrated against the 91500 standard.

In order to compare previously published datasets with the new data, all analyses have been filtered in a similar way. The data have been filtered for discordance > 10% or < –10% and relative error on age < 20% (2σ). For the new data, 66 out of 680 analyses were rejected. The detrital zircon data are visualized and analyzed by the Python-based detrital Py-package (Sharman et al., 2018). For grains < 1000 Ma, the $^{238}U/^{206}Pb$ age was used, while the $^{207}Pb/^{206}Pb$ age was used for the older grains.

Modelling Triassic sediment input and distribution

As indicated above, we have used a novel approach to reconstruct the distribution and the length of the easterly derived Triassic sediment beyond the GBSB, which was developed based on sediment budget calculations.

The well-established BQART-approach (Syvitski and Milliman, 2007; Sømme 2009), can provide an estimate of sediment supply (in mass per time) to sedimentary basins when a series of key parameters about the catchment are provided (lithology, relief, area, temperature, degree of glacial coverage and water discharge). Gilmullina et al., (2021b) compared the sediment load to the GBSB measured from the seismic data to what could be expected to have been delivered from the Uralo-Siberian source throughout the Triassic using a BQART-MCS approach to quantify and represent the uncertainty for the unknown input values. Their results showed that there was generally an excellent fit with the estimated sediment load of the sedimentary units that were fully constrained within the seismic data (Induan, Olenekian, and Carnian C1). Sediment load in late Carnian (Carnian C2, Carnian C3+4), and Norian (Norian N2) units, as determined from seismic data, are all towards the lower end of the modelled sediment loads, constituting 40, 30 and 25% of the mode of the modelled sediment loads, respectively (Fig. 6). This indicates loss of a significant amount of sediment from the GBSB, and large-scale sediment bypass distribution outside the basin can explain the documented similarities of the Upper Triassic sediments in other Arctic basins.

We assume that the difference between averages of modelled sediment loads and observed sediment loads approximate the amount of sediment that prograded over from the GBSB into adjacent sedimentary basins. The minimum width of the Arctic Basin was estimated as the distance between Svalbard and Severnaya Zemlya Archipelago, essentially the area with confirmed distribution of the Triassic sediments (Schneider et al., 1989). The maximum width of the circum-Arctic was based on the 200 m.y. reconstruction of Shepard et al. (2013). We used an average basin depth of 500 m as many of the backstripped second-order clinoform surfaces in the GBSB scale to such depths (Klausen and Helland-Hansen, 2018), and the thickness of late Triassic formations seem to have scaled to such thicknesses before post-depositional erosion (Klausen et al., 2017). Thicknesses of the second order Carnian and Norian sequences in the Sverdrup Basin are approximately 300 m and 400 m accordingly (Embry, 2011).

Estimation of the sedimentary system's progradation length was made by the following workflow: (1) the volume of missing sediments per unit was calculated as a difference between mean modelled and observed sediment load and (2) divided on the mean basin depth and (3) basin width (Table 1). This leads to a depositional model for the Arctic, which is independently verified using published and new (DR1) detrital zircon age data (Fig. 4).

Results

Estimation of bypassed sediment volumes from GBSB

The BQART model shows that the Uralo-Siberian source potentially generated 670 megatons of sediments per Myr in the Carnian (Gilmullina et al., 2021b). During the Triassic until the early Carnian, sediments from the Uralo-Siberian source were largely contained within the GBSB, but after this, sedimentary geometries show that progressively greater amounts of sediments were bypassed from the GBSB to basins to the north (Figs. 1-3). This is also seen as a progressively increasing mismatch between observed in seismic and modelled sediment load (Fig. 5, Table 1). Assuming constant sediment production in the catchment through the Carnian, seemingly reasonable based on the sedimentary geometries, $5.5*10^{9}$ MT of sediments were produced in the Uralo-Siberian source, and 68% of these sediments were bypassed into basins to the north and northwest of the GBSB.

Norian strata in the GBSB are strongly eroded, especially towards the Finnmark Platform, Loppa High and Svalbard but also locally around salt domes reactivated at the Triassic-Jurassic transition (Müller et al., 2019). Estimates of Norian sediment supply are, therefore, more uncertain than the Carnian. If the Uralo-Siberian source continued to generate the same amounts of sediments, $12.4*10^9$ MT were generated. Approximately 25% of these sediments in the GBSB were later eroded, and 64% probably bypassed to basins beyond.

How far did bypassed sediments prograde into the Arctic basins?

Using the sediment volumes calculated above, it is possible to estimate how far the sediments that bypassed the GBSB prograded into the adjacent basins. Basin geometry is approximated using a simple rectangular prism, where the width is equal to the distance between Svalbard and Severnaya Zemlya: 1400 km using reconstructions by Shephard et al. (2013). Prism height equals average basin depth, approximated by the decompacted sediment thicknesses in the Sverdrup Basin. Average thicknesses of Late Triassic deposits in the Sverdrup Basin are up to c. 400 m, which translates to thicknesses of 700 m (DR1) when applying similar decompaction parameters and methodology as used in a study on time-equivalent strata in the Barents Sea by Klausen and Helland-Hansen (2018).

Using this simple model, the mean progradation lengths of bypassed sediments beyond the GBSB becomes 1300 km for the Carnian, and 4500 km for the Norian (DR1) (Fig. 1a, 5). This implies that sediments from the Uralo-Siberian source, bypassing the GBSB, could have supplied sediment through nearly the entire Sverdrup Basin in the Carnian, and all the way to Arctic Alaska in the Norian.

Are these progradation lengths supported by detrital zircon data?

Calculated progradation lengths are supported by a compilation of new and previously published detrital zircon age data in the Triassic basins throughout the Arctic (Figs. 4-5). These detrital zircon age spectra show that most areas are dominated by locally derived sediments (strong pre-500 Ma peaks) in the Early and Middle Triassic (Bue and Andresen, 2014; Anfinson et al., 2016; Gottlieb et al., 2014), until the prograding sedimentary system from the Uralo-Siberian source arrives at different times in different locations (Eide et al., 2018; Figs. 8-11).

The Uralo-Siberian source sediment is characterized by the large group of young zircons (30% of all zircons) along with other distinctive Uralian source zircons with a time span between 600 and 250 Myr (Figs.4a-c, 8; Klausen et al., 2017; Fleming et al., 2016; Flowerdew et al. 2019; Sirevaag in prep.). However, because very few to no detrital zircon age spectra from Carnian fluvial rocks are published from the northern part of the Ural Foreland and the NE parts of the Siberian source, it is difficult to know whether we are dealing with temporal change to younger zircons in both areas or that the two areas have distinct signatures. If they do have distinct signatures and the signature of the Ural Foreland in the Carnian is approximated by the signature found in Chistyakova et al., (2020). It is very likely that the typical Ladinian-early Carnian succession in the GBSB is characterized by a detrital zircon age spectrum with Permian age grains, and that the Triassic grains are typical for the late Carnian to-Late Triassic successions. The fact that the youngest grains have crystallization ages close to the depositional age of the stratigraphic units in which they are found suggest that the source is volcanic and active shortly before or during deposition, and the tectonically active Novaya Zemlya Fold and Thrust Belt at the perimeter of the Siberian traps and in the northern continuation of the Urals is one suggested candidate (Klausen et al., 2017), together with more deep-rooted Triassic intrusions widely spread in West Siberia and CAOB, albeit at more distance from the GBSB (Tevelev, 2013).

In areas close to the Uralo-Siberian source, such as the Finnmark Platform (Figs. 4d, 8), locally derived sediments were already replaced by sediments from the Uralo-Siberian source in the Induan (Early Triassic). The Uralo-Siberian source-signature is characteristic of the succession in Chukotka throughout the Triassic, indicating that it was located close to this provenance throughout the Triassic. In medial areas, such as Svalbard, locally derived sediments persist until sediments from the Uralo-Siberian source arrive in the earliest Carnian (C1, Fig. 3, 4e-f). At all investigated areas, including the Sverdrup Basin (Fig. 1), an incursion of a mudstone-rich sedimentary system with sparse fine-grained sandstones with a typical Uralo-Siberian source detrital zircon signature occurs in the Late Carnian (Figs.4j-k, 9). In Arctic Alaska, locally derived zircon age spectra are observed in the Norian (Figs. 4s, 8, 9), but the characteristic young Uralo-Siberian source signature becomes mixed in with the local signal in the late Norian (Figs. 4r, 10) suggesting that the system reached all the way to Arctic Alaska. This distribution of detrital zircon ages fits excellently with calculated progradation lengths of bypassed Uralo-Siberian source sediment for each unit prograding sequentially from the GBSB (Fig. 1).

Discussion

Implications for plate-tectonic reconstructions

Looking at the current basin structure in the Arctic, the youngest ocean basin is the early Cenozoic to Recent Eurasia Basin (Fig. 12). Before this basin opened, the Lomonosov Ridge is reconstructed at the edge of the Barents Shelf. The earlier phase of opening formed the Amerasia Basin in the Cretaceous, but the lack of magnetic anomalies (Gaina et al., 2011 Zhang et al., 2019) and good understanding of the kinematics of the opening makes it difficult to choose one unique paleogeographic model for what the Arctic looked like prior to rifting. This is where the new data base on the GBSB can play an important role.

The model for sediment dispersal presented above has a set of implications for plate-tectonic reconstructions in the Arctic:

The sedimentary record of the Chukotka Basin follows the same sediment supply trend and contains late Palaeozoic and Triassic zircons best explained by bypass from a Uralo-Siberian source throughout the Triassic (Figs. 8-11). This implies a close docking of the Lomonosov Ridge against the northern GBSB, and Chukotka docked close to the Lomonosov Ridge, as suggested by Miller et al. (2013, 2018; Fig. 1a). Chukotka is then located closer to the GBSB (different from Nikishin et al., 2019) and rotated more compared to Shephard et al. (2013) and Sømme et al. (2018) (Fig. 12). The GBSB and Greenland blocks were in that case located very close to the Sverdrup Basin (Fig. 12).

The East Siberian Sea shelf, including New Siberian Islands (NSI), is one of the most complex areas in the Arctic (Piepjohn et al., 2018, Prokopiev et al., 2018). The pre-breakup location of the NSI and its affiliation to Arctic or Siberia is disputed (Kuzmichev, 2009, Ershova et al., 2015). The NSI deposits represented the deepest and most distal facies of the Uralo-Siberian system throughout the Triassic (Figs. 8-11, Egorov et al., 1987; Zakharov et al., 2010). Thus, a position of the NSI adjacent to the Sverdrup Basin or Severnaya Zemlya/GBSB is unlikely because these areas are dominated by fluvial deposits in the Carnian and late Norian (Figs. 9-10). Only very distal facies, mainly thinly bedded shales with carbonate interbeds, are present during these times in the NSI. In order to deposit such distal deposits and still contain zircons with a Uralian signature, the location of the NSI must have been far offset from the main sediment transportation route, in more distal locations in line with suggestions made by

Nikishin et al. (2019, Fig 1). The precise Triassic location of the NSI remains to be resolved and is an interesting topic for future study.

Location of Arctic Alaska near Laurentia (Miller et al., 2013, Nikishin et al., 2019, Shepard et al., 2013; Drøssing et al., 2020; McClelland et al., 2021) is the least controversial among reconstructed terranes; however, the angle of rotation of the continent, associated with Amerasia Basin opening, is very different from author to author (Fig. 1). Distribution of sedimentary environments and published detrital zircon data support a rotation of Arctic Alaska as suggested by Shephard (2013) and Gottlieb et al. (2014). Such a rotation is in accordance with the fact that sediments with an Uralo-Siberian source-signature are only found in the Lisburne Hills in the SW part of Arctic Alaska (Fig. 4r and 10).

During the Carnian – Norian, the Arctic basins (GBSB, Sverdrup, Chukotka, New Siberian Island, Wrangel Island, Alaska) received clastic sediments with a significant group of zircons with ages close to the depositional age (Fig. 4, Flowerdew et al., 2019, Miller et al., 2013). Many studies discussed the origin of this zircons and suggested different potential sources such as Taimyr (Omma et al., 2011; Fleming et al., 2016), the "Pangean Rim of Fire" or a subduction zone along the western margin of Laurentia (Hadlari et al., 2018). Our results also imply that the presence of these "young" zircons in the Upper Triassic deposits do not argue in favour of a magmatic arc system (e.g., Hadlari et al., 2017 Midwinter et al., 2016) extending all the way into the Arctic region. This is because similar zircon age populations were produced by the Uralo-Siberian source (Figs. 8-11; Tevelev, 2013, Klausen et al., 2017; Gilmullina et al., 2021b), and because sedimentary systems sourced from the Urals and Siberia, and prograding northwestwards across the GBSB into the wider Arctic, are the most likely prime cause of the Triassic zircon distribution.

Is Crockerland a necessary concept in the Triassic?

The Crockerland terrane is a hypothetical landmass proposed to explain the facies distribution in Svalbard and the Sverdrup Basin (Fig. 1; Embry et al., 1993). There are, however, numerous problems with this suggestion: Firstly, clinoforms in the GBSB show sediment transport towards the NW (Riis et al., 2008; Glørstad-Clark et al., 2010; Gilmullina er al., 2021a), the Late Triassic channels in the GBSB and Svalbard also show sediment transport towards the NW (Klausen and Mørk, 2014; Haile et al., 2018) which implies that sediment was transported from the Uralo-Siberian source across the Barents Sea over Svalbard throughout the Late Triassic in a direction trending directly towards where the Sverdrup Basin was located (Miller et al., 2013; Gilmullina et al., 2021a). The deep basin that was situated between Uralo-Siberian source and Laurentia-Greenland, accommodated thick, organic-rich marine shales of the Middle Triassic Steinkobbe, Botneheia and Murray Harbor formations, until the basin was finally filled in the Late Triassic. Secondly, large amounts of sediments prograded over to basins to the NW (Fig. 6) (Klausen et al., 2019), and results of the modelling presented here show the potential for the Uralo-Siberian sediment source to supply clastic material across many hundreds of kilometres.

In addition, the relatively short distance between the GBSB, Svalbard and the Sverdrup Basin throughout the Triassic (Fig. 1) (Shepard et al., 2013) and the late Carnian and late Norian timing of bypass in the GBSB coincide with the timing of the Pat Bay/Hoyle Bay formations (Fig. 3) in the Sverdrup Basin. Thirdly, it is unlikely that a very proximal landmass would supply the fine-grained and well-sorted sandstones observed in the Sverdrup Basin, and no evidence for a northern source or southerly transport directions is observed in time-equivalent strata on Svalbard (e.g., Riis et al., 2008; Gilmullina et al., 2021a). Finally, the great similarity between the detrital zircon age spectra in the late Carnian and Late Norian of the Sverdrup Basin (Fig.

4j, k) and the GBSB, including Svalbard, shows that the two basins had a common Uralo-Siberian source.

The Urals, Taimyr and Siberia have been suggested as a source for the Triassic sediments in the Sverdrup Basin in previous studies (Omma et al., 2011, 2009; Anfinson et al., 2016; Miller et al., 2013), and the GBSB has even been proposed as an alternative pathway for sediment transport (Anfinson et al., 2016). Our data add weight to the idea that the Uralo-Siberian source is the primary source for the Late Triassic sediments in Arctic basins, and that the GBSB is the main sediment route throughout which the bypass took place (Figs. 9-10).

Based on the evidence presented above, we suggest that there is no need for an extra sediment source in the middle of the Triassic Arctic, as shown in many reconstructions as a Chukotka-Alaska microcontinent (Sømme et al., 2018) or as local highs (Miller et al., 2018). In fact, inferring such a terrane sets up an artificial constraint on sediment dispersal patterns and plate reconstructions because models need to account for an "Arctic Atlantis". We propose that the Crockerland concept be abandoned, that a more useful view is that the Arctic basins were connected in the Triassic, and that the Polar Urals together with source areas in West Siberia supplied the majority of the basin-filling sediment, vast amounts of mudstone-rich sediments with mineralogically immature sandstones and a characteristic detrital zircon age spectrum.

Conclusions

In this study, we present a novel approach, based on sediment budget modelling and support from provenance data, that helps to constrain sediment transport pathways and improve plate tectonic and paleogeographic reconstruction. The source-to-sink approach shows the importance of evaluating sediment bypass and the connectedness of adjacent sedimentary basins, and of using a mass balance approach. Based on this work, we have made suggestions to the Triassic plate tectonic reconstruction of the Arctic, although this interpretation should be tempered by the fact that this is essentially a sedimentological, not geodynamic approach. Future work would ideally include a rigorous geodynamic testing of the ideas presented.

The present study presents a revised, uniform Triassic lithostratigraphy for the Arctic, explaining the sediment supply patterns that created the characteristic detrital zircon spectra found throughout the Triassic within the Arctic sedimentary basins. Results show that the Uralo-Siberian signature was found in detrital zircons across all basins in the Carnian and the Norian, which implies that the Arctic basins were closely connected.

The results imply that the Uralo-Siberian source dominated the Arctic basins in the Late Triassic, and that enigmatic local terranes such as the “Crockerland” or the Boreal “Ring of Fire” are superfluous sediment sources not needed to explain Arctic sediment supply. Finally, we show how the reconstructed Arctic sediment routing system constrains plate tectonic models and offer new plate tectonic and paleogeographic reconstructions based on this concept.

Acknowledgments

We acknowledge the Norwegian Research Council for funding through the Petromaks2-program to the ISBAR (267689) and FueBAR (308799) projects. Anna Suslova acknowledges the Russian Foundation for Basic Research for funding through project No 20-55-20007. We thank Elizabeth Miller and Amanda Owen for important discussions and constructive comments. PGS, TGS, the Norwegian Petroleum Directorate are acknowledged for providing seismic data and for permission to publish seismic lines. We also thank Schlumberger for access to Petrel under an educational license to the University of Bergen.

References

Anfinson, O. A., Embry, A. F., and Stockli, D. F., 2016, Geochronologic constraints on the Permian–Triassic northern source region of the Sverdrup Basin, Canadian Arctic Islands: Tectonophysics, v. 691, p. 206-219. https://doi.org/10.1016/j.tecto.2016.02.041

Bergan, M., and Knarud, R., 1993, Apparent changes in clastic mineralogy of the Triassic–Jurassic succession, Norwegian Barents Sea: Possible implications for palaeodrainage and subsidence, in Vorren, T.O., Bergsager, E., Dahl-Stamnes, Ø.A., Holter, E., Johansen, B., Lie, E., and Lund, T.B., eds., Norwegian Petroleum Society Special Publication, Volume 2: Amsterdam, Elsevier, p. 481–493, https://doi .org/10.1016/B978-0-444-88943-0.50034-4.

Bue, P. E., and Andresen, A., 2014, Constraining depositional models in the Barents Sea region using detrital zircon U–Pb data from Mesozoic sediments in Svalbard: Geological Society, London, Special Publications, v. 386, no. 1, p. 261-279. http://dx.doi.org/10.1144/SP386.14

Chistyakova, A. V., Veselovskiy, R. V., Semenova, D. V., Kovach, V. P., Adamskaya, E. V., & Fetisova, A. M. (2020, May). Stratigraphic Correlation of Permian–Triassic Red Beds, Moscow Basin, East European Platform: First Detrital Zircon U–Pb Dating Results. In Doklady Earth Sciences (Vol. 492, No. 1, pp. 306-310). Pleiades Publishing.

Colpron, M., & Nelson, J. L., 2011. A Palaeozoic NW Passage and the Timanian, Caledonian and Uralian connections of some exotic terranes in the North American Cordillera. Geological Society, London, Memoirs, 35(1), 463-484. https://doi.org/10.1144/M35.31

Czarniecka, U., Haile, B. G., Braathen, A., Krajewski, K. P., Kristoffersen, M., Jokubauskas, P., Kurapov, M., Ershova, V., Khudoley, A., and Makariev, A., Petrography, bulk-rock geochemistry, detrital zircon U–Pb geochronology and Hf isotope analysis for constraining provenance: An example from Middle Triassic deposits (Bravaisberget Formation), Sørkappøya, Svalbard. https://dx.doi.org/10.17850/njg100-3-5

Doré, A. G., Lundin, E. R., Gibbons, A., Sømme, T. O., & Tørudbakken, B. O. (2016). Transform margins of the Arctic: a synthesis and re-evaluation. Geological Society, London, Special Publications, 431(1), 63-94. https://doi.org/10.1144/SP431.8

Døssing, A., Gaina, C., Jackson, H. R., & Andersen, O. B. (2020). Cretaceous ocean formation in the High Arctic. Earth and Planetary Science Letters, 551, 116552. https://doi.org/10.1016/j.epsl.2020.116552

Egorov, A. U., Bogomolov, Y. A., Konstantinov, A. G., et al., 1987. Stratigraphy of Triassic deposits of Kotelny Island (Novosibirsk Islands) (In Russian). Boreal Triassic: 66-80

Eide, C. H., Klausen, T. G., Katkov, D., Suslova, A. A., and Helland-Hansen, W., 2018, Linking an Early Triassic delta to antecedent topography: Source-to-sink study of the southwestern Barents Sea margin: GSA Bulletin, v. 130, no. 1-2, p. 263-283. https://doi.org/10.1130/B31639.1

Embry, A., 1997, The Blind Fiord Formation and Blaa Mountain Group (Triassic) of northwestern Axel Heiberg Island, Canadian Arctic Archipelago: Geological Survey of Canada, Paper, v. 97, p. 193-198. https://doi.org/10.1130/B31639.1

Embry, A., and Beauchamp, B., 2019, Chapter 14 - Sverdrup Basin, *in* Miall, A. D., ed., The Sedimentary Basins of the United States and Canada (Second Edition), Elsevier, p. 559-592. https://doi.org/10.1016/B978-0-444-63895-3.00014-0

Embry, A. F., 1993, Crockerland — the northwest source area for the Sverdrup Basin, Canadian Arctic Islands, *in* Vorren, T. O., Bergsager, E., Dahl-Stamnes, Ø. A., Holter, E., Johansen, B., Lie, E., and Lund, T. B., eds., Norwegian Petroleum Society Special Publications, Volume 2, Elsevier, p. 205-216. https://doi.org/10.1016/B978-0-444-88943-0.50018-6

Ershova, V. B., Prokopiev, A. V., Khudoley, A. K., Sobolev, N. N., & Petrov, E. O. (2015). U/Pb dating of detrital zircons from late Palaeozoic deposits of Bel'kovsky Island (New Siberian Islands): Critical testing of Arctic tectonic models. International Geology Review, 57(2), 199-210. https://doi.org/10.1080/00206814.2014.999358

Fleming, E. J., Flowerdew, M. J., Smyth, H. R., Scott, R. A., Morton, A. C., Omma, J. E., Frei, D., and Whitehouse, M. J., 2016, Provenance of Triassic sandstones on the southwest Barents Shelf and the implication for sediment dispersal patterns in northwest Pangaea: Marine and Petroleum Geology, v. 78, p. 516-535. https://doi.org/10.1016/j.marpetgeo.2016.10.005

Flowerdew, M. J., Fleming, E. J., Morton, A. C., Frei, D., Chew, D. M., and Daly, J. S., 2019, Assessing mineral fertility and bias in sedimentary provenance studies: examples from the Barents Shelf: Geological Society, London, Special Publications, v. 484, p. SP484. 411. https://doi.org/10.1144/SP484.11

Galloway, B. J., Dewing, K., Beauchamp, B., & Matthews, W. 2021. Upper Paleozoic stratigraphy and detrital zircon geochronology along the northwest margin of the Sverdrup Basin, Arctic Canada: insight into the paleogeographic and tectonic evolution of Crockerland. Canadian Journal of Earth Sciences, 58(2), 164-187. https://doi.org/10.1139/cjes-2019-0226

Gaina, C., Werner, S. C., Saltus, R., & Maus, S. (2011). Circum-Arctic mapping project: new magnetic and gravity anomaly maps of the Arctic. Geological Society, London, Memoirs, 35(1), 39-48.

Gilmullina, A., Klausen, T. G., Paterson, N. W., Suslova, A., and Eide, C. H., 2021a, Regional correlation and seismic stratigraphy of Triassic Strata in the Greater Barents Sea: Implications for sediment transport in Arctic basins: *Basin Res. 2021; 33: 1546– 1579* https://doi.org/10.1111/bre.12526

Gilmullina, A., Klausen, T. G., Doré, A. G., Rossi, V. M., Suslova, A., & Eide, C. H., 2021b. Linking sediment supply variations and tectonic evolution in deep time, source-to-sink systems—The Triassic Greater Barents Sea Basin. GSA Bulletin.

Glørstad-Clark, E., Faleide, J. I., Lundschien, B. A., & Nystuen, J. P. (2010). Triassic seismic sequence stratigraphy and paleogeography of the western Barents Sea area. Marine and Petroleum Geology, 27(7), 1448–1475. https://doi.org/10.1016/j.marpetgeo.2010.02.008

Gottlieb, E. S., Meisling, K. E., Miller, E. L., and Mull, C. G. G., 2014, Closing the Canada Basin: Detrital zircon geochronology relationships between the North Slope of Arctic Alaska and the Franklinian mobile belt of Arctic Canada: Geosphere, v. 10, no. 6, p. 1366-1384. https://doi.org/10.1130/GES01027.1

Hadlari, T., Midwinter, D., Poulton, T. P., and Matthews, W. A., 2017, A Pangean rim of fire: Reviewing the Triassic of western Laurentia: Lithosphere, v. 9, no. 4, p. 579-582. https://doi.org/10.1130/L643.1

Haile, B. G., Klausen, T. G., Jahren, J., Braathen, A., & Hellevang, H. (2018). Thermal history of a Triassic sedimentary sequence verified by a multi-method approach: Edgeøya, Svalbard, Norway. Basin Research, 30(6), 1075-1097. https://doi.org/10.1111/bre.12292

Houseknecht, D. W., 2019, Evolution of the Arctic Alaska sedimentary basin, The sedimentary basins of the United States and Canada, Elsevier, p. 719-745. https://doi.org/10.1016/B978-0-444-63895-3.00018-8

Jackson, S.E., Pearson, N.J., Griffin, W.L. and Belousova, E.A. (2004) The application of laser ablation-inductively coupled plasma-mass spectrometry to in situ U-Pb zircon geochronology. Chem. Geol., 211, 47–69.

Jakobsson, M., R. Macnab, L. Mayer, R. Anderson, M. Edwards, J. Hatzky, H. W. Schenke, and P. Johnson (2008), An improved bathymetric portrayal of the Arctic Ocean: Implications for ocean modeling and geological, geophysical and oceanographic analyses, Geophysical Research Letters, https://doi.org/10.1029/2008GL033520

Klausen, T. G., and Helland-Hansen, W., 2018, Methods For Restoring and Describing Ancient Clinoform Surfaces: Journal of Sedimentary Research, v. 88, no. 2, p. 241-259. https://doi.org/10.2110/jsr.2018.8

Klausen, T. G., & Mørk, A. (2014). The Upper Triassic paralic deposits of the De Geerdalen Formation on Hopen: outcrop analog to the subsurface Snadd Formation in the Barents Sea. AAPG Bulletin, 98(10), 1911-1941. https://doi.org/10.1306/02191413064

Klausen, T. G., Müller, R., Slama, J., and Helland-Hansen, W., 2017, Evidence for Late Triassic provenance areas and Early Jurassic sediment supply turnover in the Barents Sea Basin of northern Pangea: Lithosphere, v. 9, no. 1, p. 14-28. https://doi.org/10.1130/L556.1

Klausen, T. G., Nyberg, B., and Helland-Hansen, W., 2019, The largest delta plain in Earth's history: Geology, v. 47, no. 5, p. 470-474. https://doi.org/10.2110/jsr.2018.8

Klausen, T. G., Ryseth, A. E., Helland-Hansen, W., Gawthorpe, R., and Laursen, I., 2015, Regional development and sequence stratigraphy of the Middle to Late Triassic Snadd formation, Norwegian Barents Sea: Marine and Petroleum Geology, v. 62, p. 102-122. https://doi.org/10.1016/j.marpetgeo.2015.02.004

Klausen T.G., Rismyhr B., Müller R., Olaussen S. Changing provenance and stratigraphic signatures across the Triassic – Jurassic boundary in eastern Spitsbergen and the subsurface Barents Sea, Norwegian Journal of Geology, in press.

Krajewski, K., 2008, The Botneheia Formation (Middle Triassic) in Edgeøya and Barentsøya, Svalbard: lithostratigraphy, facies, phosphogenesis, paleoenvironment: Polish Polar Research, v. 29, p. 319–364.

Krajewski, K. P., & Weitschat, W. 2015, Depositional history of the youngest strata of the Sassendalen Group (Bravaisberget Formation, Middle Triassic–Carnian) in southern Spitsbergen, Svalbard. In Annales Societatis Geologorum Poloniae (Vol. 85, No. 1, pp. 151-175). https://doi.org/10.14241/asgp.2014.005

Kuzmichev, A. B., & Pease, V. L. (2007). Siberian trap magmatism on the New Siberian Islands: constraints for Arctic Mesozoic plate tectonic reconstructions. Journal of the Geological Society, 164(5), 959-968. https://doi.org/10.1144/0016-76492006-090

Lord, G., Solvi, K. H., Ask, M., Mork, A., Hounslow, M., & Paterson, N. W. (2014). The Hopen member: a new member of the triassic de Geerdalen formation. Norwegian petroleum directorate Bulletin, 11, 81-96.

McClelland, W. C., Strauss, J. V., Colpron, M., Gilotti, J. A., Faehnrich, K., Malone, S. J., Gehrels, G. E., Macdonald, F. A., & Oldow, J. S. (2021). 'Taters versus sliders: Evidence for a long-lived history of strike-slip displacement along the canadian arctic transform system (CATS). GSA Today, 31(7), 4–11. 10.1130/GSATG500A.1

Midwinter, D., Hadlari, T., Davis, W. J., Dewing, K., & Arnott, R. W. C. (2016). Dual provenance signatures of the Triassic northern Laurentian margin from detrital-zircon U-Pb and Hf-isotope analysis of Triassic–Jurassic strata in the Sverdrup Basin. Lithosphere, 8(6), 668-683.

Miller, E. L., Meisling, K. E., Akinin, V. V., Brumley, K., Coakley, B. J., Gottlieb, E. S., Hoiland, C. W., Brien, T. M., Soboleva, A., and Toro, J., 2018, Circum-Arctic Lithosphere Evolution (CALE) Transect C: displacement of the Arctic Alaska–Chukotka microplate towards the Pacific during opening of the Amerasia Basin of the Arctic: Geological Society, London, Special Publications, v. 460, no. 1, p. 57. https://doi.org/10.1144/SP460.9

Miller, E. L., Soloviev, A. V., Prokopiev, A. V., Toro, J., Harris, D., Kuzmichev, A. B., & Gehrels, G. E. (2013). Triassic river systems and the paleo-Pacific margin of northwestern Pangea. Gondwana Research, 23(4), 1631–1645. https://doi.org/10.1016/j.gr.2012.08.015

Miller, E. L., Toro, J., Gehrels, G., Amato, J. M., Prokopiev, A., Tuchkova, M. I., Akinin, V. V., Dumitru, T. A., Moore, T. E., and Cecile, M. P., 2006, New insights into Arctic paleogeography and tectonics from U-Pb detrital zircon geochronology: Tectonics, v. 25, no. 3. https://doi.org/10.1029/2005TC001830

Moore, T. E., Dumitru, T. A., Adams, K. E., Witebsky, S. N., Harris, A. G., Miller, E., Grantz, A., and Klemperer, S., 2002, Origin of the Lisburne Hills-Herald Arch structural belt: Stratigraphic, structural, and fission-track evidence from the Cape Lisburne area, northwestern Alaska: SPECIAL PAPERS-GEOLOGICAL SOCIETY OF AMERICA, p. 77-110.

Mozley, P. S., and Hoernle, K., 1990, Geochemistry of carbonate cements in the Sag River and Shublik Formations (Triassic/Jurassic), North Slope, Alaska: implications for the geochemical evolution of formation waters: Sedimentology, v. 37, no. 5, p. 817-836. https://doi.org/10.1111/j.1365-3091.1990.tb01827.x

Mørk, A., Embry, A. F., and Weitschat, W., 1989, Triassic transgressive-regressive cycles in the Sverdrup Basin, Svalbard and the Barents Shelf, Correlation in hydrocarbon exploration, Springer, p. 113-130.¨

Müller, R., Klausen, T.G., Faleide, J.I., Olaussen, S., Eide, C.H., and Suslovad, A., 2019, Linking regional unconformities in the Barents Sea to compression-induced forebulge uplift at the Triassic-Jurassic transition: Tectonophysics, v. 765, p. 35–51, https://doi .org/10.1016/j.tecto.2019.04.006.

Nikishin, A. M., Petrov, E. I., Cloetingh, S., Freiman, S. I., Malyshev, N. A., Morozov, A. F., Posamentier, H. W., Verzhbitsky, V. E., Zhukov, N. N., and Startseva, K., 2019, Geological structure and history of the Arctic Ocean based on new geophysical data: Implications for paleoenvironment and paleoclimate. Part 2. Mesozoic to Cenozoic geological evolution: Earth-Science Reviews, p. 103034. https://doi.org/10.1016/j.earscirev.2019.103034

Omma, J., Pease, V., and Scott, R., 2011, U–Pb SIMS zircon geochronology of Triassic and Jurassic sandstones on northwestern Axel Heiberg Island, northern Sverdrup Basin, Arctic Canada: Geological Society, London, Memoirs, v. 35, no. 1, p. 559-566. https://doi.org/10.1144/M35.37

Paton, C., Woodhead, J.D., Hellstrom, J.C., Hergt, J.M., Greig, A. and Maas, R. (2010) Improved laser ablation U-Pb zircon geochronology through robust downhole fractionation correction. Geochemistry, Geophys Geosystems. doi: 10.1029/2009GC002618

Petrus, J.A. and Kamber, B.S. (2012) VizualAge: A Novel Approach to Laser Ablation ICP-MS U-Pb Geochronology Data Reduction. Geostand. Geoanalytical Res., 36, 247–270.

Piepjohn, K., Lorenz, H., Franke, D., et al., 2018. Mesozoic structural evolution of the New Siberian Islands. Geological Society, London, Special Publications, 460(1): 239-262 https://doi.org/10.1144/SP460.1

Prokopiev Andrei V., Victoria B. Ershova, Owen Anfinson, Daniel Stockli, Jeremy Powell, Andrei K. Khudoley, Dmitry A. Vasiliev, Nikolay N. Sobolev, Eugeny O. Petrov, Tectonics of the New Siberian Islands archipelago: Structural styles and low-temperature thermochronology, Journal of Geodynamics, Volume 121, 2018, Pages 155-184, https://doi.org/10.1016/j.jog.2018.09.001

Richardson, J., Hodgson, D., Paton, D., Craven, B., Rawcliffe, A., and Lang, A., 2017, Where is my sink? Reconstruction of landscape development in southwestern Africa since the Late Jurassic: Gondwana Research, v. 45, p. 43-64. https://doi.org/10.1016/j.gr.2017.01.004

Riis, F., Lundschien, B. A., Høy, T., Mørk, A., & Mørk, M. B. E. (2008). Evolution of the Triassic shelf in the northern Barents Sea region. Polar Research, 27(3), 318-338. DOI: 10.1111/j.1751-8369.2008.00086.x

Rossi, V. M., Paterson, N. W., Helland-Hansen, W., Klausen, T. G., & Eide, C. H. (2019). Mud-rich delta-scale compound clinoforms in the Triassic shelf of northern Pangea (Havert Formation, southwestern Barents Sea). Sedimentology, 66(6), 2234–2267.

Sláma, J., Košler, J., Condon, D.J., Crowley, J.L., Gerdes, A., Hanchar, J.M., Horstwood, M.S.A., Morris, G.A., Nasdala, L., Norberg, N., Schaltegger, U., Schoene, B., Tubrett, M.N. and Whitehouse, M.J. (2008) Plešovice zircon - A new natural reference material for U-Pb and Hf isotopic microanalysis. Chem. Geol., 249, 1–35.

Shephard, G., Müller, D., and Seton, M., 2013, The tectonic evolution of the Arctic since Pangea breakup: Integrating constraints from surface geology and geophysics with mantle structure: Earth-Science Reviews, v. 124, p. 148-183. https://doi.org/10.1016/j.earscirev.2013.05.012

Schneider, G. V., Efremova, V. I., & Sedov, V. N. (1989). Stratigraphy and formation conditions of the Mesozoic deposits of the northeastern tip of the Taimyr Peninsula. Geological structure and minerals of the northeastern tip of the Taimyr Peninsula. L .: PGO "Sevmorgeologiya", 22-34.(in Russian)

Soloviev, A., Zaionchek, A., Suprunenko, O., Brekke, H., Faleide, J., Rozhkova, D., Khisamutdinova, A., Stolbov, N., and Hourigan, J., 2015, Evolution of the provenances of Triassic rocks in Franz Josef Land: U/Pb LA-ICP-MS dating of the detrital zircon from Well Severnaya: Lithology and Mineral Resources, v. 50, no. 2, p. 102-116.

Sømme, T., Dore, A., Lundin, E., and Tørudbakken, B., 2018, Triassic–Paleogene paleogeography of the Arctic: Implications for sediment routing and basin fill: AAPG Bulletin, v. 102, p. 2481-2517. https://doi.org/10.1306/05111817254

Sømme, T.O., Helland-Hansen, W., Martinsen, O.J., and Thurmond, J.B., 2009, Relationships between morphological and sedimentological parameters in source-to-sink systems: A basis for predicting semiquantitative characteristics in subsurface systems: Basin Research, v. 21, no. 4, p. 361–387, https://doi.org/10.1111/ j.1365-2117.2009.00397.x.

Syvitski, J.P., and Milliman, J.D., 2007, Geology, geography, and humans battle for dominance over the delivery of fluvial sediment to the coastal ocean: The Journal of Geology, v. 115, no. 1, p. 1–19, https://doi .org/10.1086/509246.

Tevelev, A. V., 2013, Types of posttrappe hypabyssal granitoids of the Circum-Siberian belt (In Russian): Moscow University Bulletin. Series 4. Geology, no. 4.

Tuchkova, M., AV, P., Khudoley, A., and VE, V., 2011, Comparative Analysis of Triassic Sedimentation in Western Chukotka and South-Eastern Side of Kular-Nera Slate Belt (Eastern Verkhoyansk region) (In Russian): Uchenye Zapiski Kazanskogo Universiteta. Seriya Estestvennye Nauki, v. 153, no. 4. https://doi.org/10.5194/smsps-4-177-2009

Tuchkova, M., Sokolov, S., and Kravchenko-Berezhnoy, I., 2009, Provenance analysis and tectonic setting of the Triassic clastic deposits in western Chukotka, northeast Russia: Stephan Mueller Special Publication Series, v. 4, p. 177-200.

Tye, R. S., Bhattacharya, J. P., Lorsong, J. A., Sindelar, S. T., Knock, D. G., Puls, D. D., & Levinson, R. A., 1999. Geology and stratigraphy of fluvio-deltaic deposits in the Ivishak Formation: Applications for development of Prudhoe Bay Field, Alaska. AAPG bulletin, 83(10), 1588-1623.

Wiedenbeck, M., Allé, P., Corfu, F., Griffin, W.L., Meier, M., Oberli, F., von Quadt, A., Roddick, J.C. and Spiegel, W. (1995) Three Natural Zircon Standards for U-Th-Pb, Lu-Hf, Trace Element and Ree Analyses. Geostand. Newsl., 19, 1–23.

Whidden, K. J., Dumoulin, J. A., & Rouse, W. A. (2018). A revised Triassic stratigraphic framework for the Arctic Alaska Basin. AAPG Bulletin, 102(7), 1171-1212. https://doi.org/10.1306/0726171616517250

Zakharov, V. A., Rogov, M., and Bragin, N., 2010, The Russian Arctic during the Mesozoic: stratigraphy, biogeography, paleogeography, and paleoclimate: Russia's Contribution to the International Polar Year 2007/08: Lithospheric Structure and Evolution. Paulsen Ed., p. 331-383.

Zhang, T., Dyment, J., & Gao, J. Y. (2019). Age of the Canada Basin, Arctic Ocean: indications from high-resolution magnetic data. Geophysical Research Letters, 46(23), 13712-13721.

Table 1. Main inputs for calculation of possible distance that the Late Triassic prograded beyond the GBSB modern boundaries

Unit	Seismic	MCS BQART, mean	Missing	Density	Age/Duration	Volume		Basin width	Basin depth	**Distance**
						Per year	Total			
	Mt/year	Mt/year	Mt/year	t/km^3	years	km^3/year	km^3	km	km	**km**
C3+4	252	688	436	2,5*10^9	6000000	0,1744	1 046 400	1400	0,5	**1 500**
N2	170	688	518	2,5*10^9	18500000	0,2072	3 833 200	1400	0,5	**5 500**

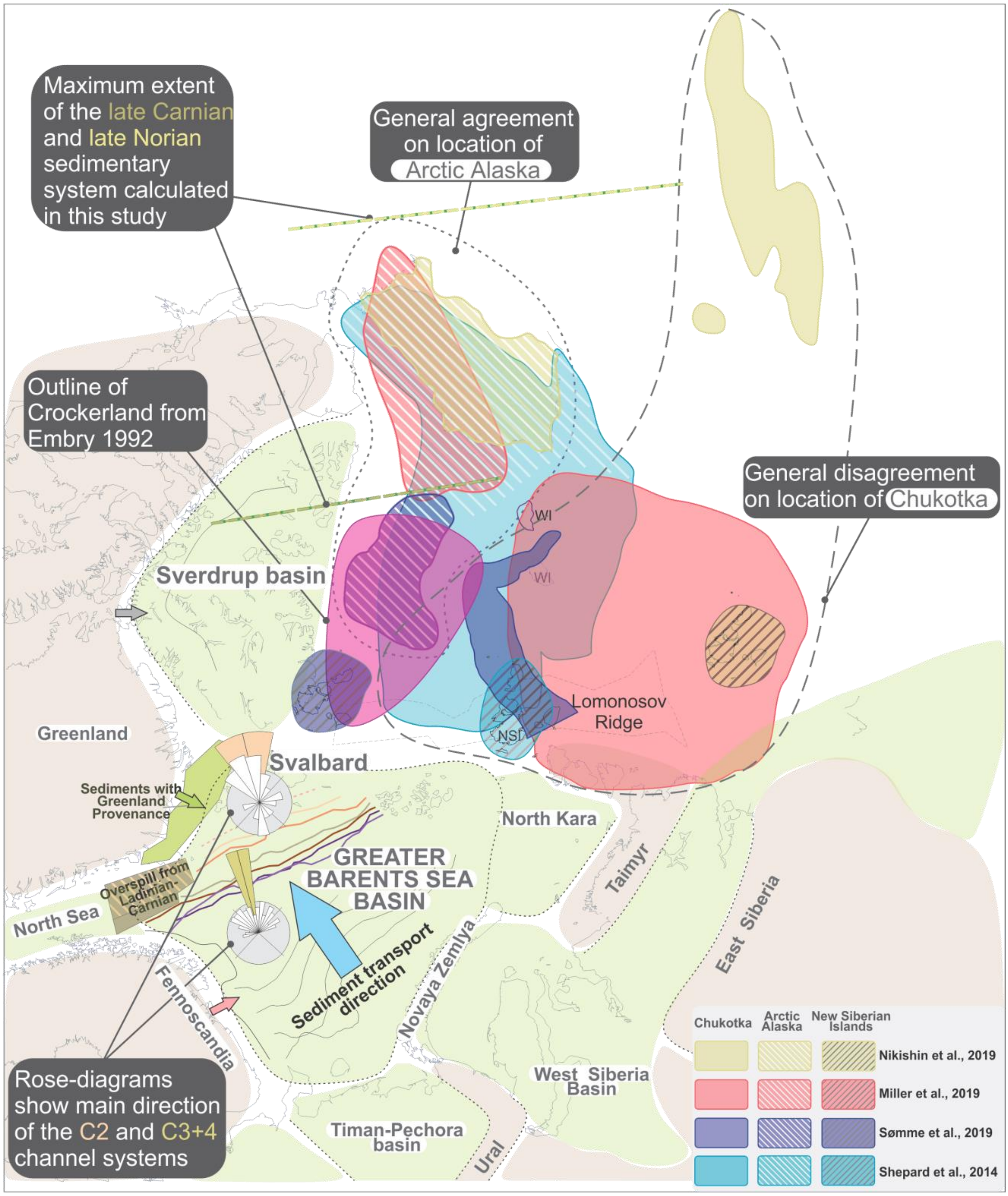

Figure 1: Overview of the main Triassic sedimentary basins, tectonic elements and sediment source areas referred to in this study and their location during the Triassic. The figure also shows recently proposed locations of the more controversial tectonic elements (Chukotka, Arctic Alaska, New Siberian Islands) and the location of the hypothetical Crockerland landmass. Triassic sediment transport directions in the Greater Barents Sea measured from clinoform belt directions (coloured lines) and fluvial channels (rose diagrams) are also shown, and these data indicate strong NW-directed sediment supply from W Russia to the Barents Sea and beyond.

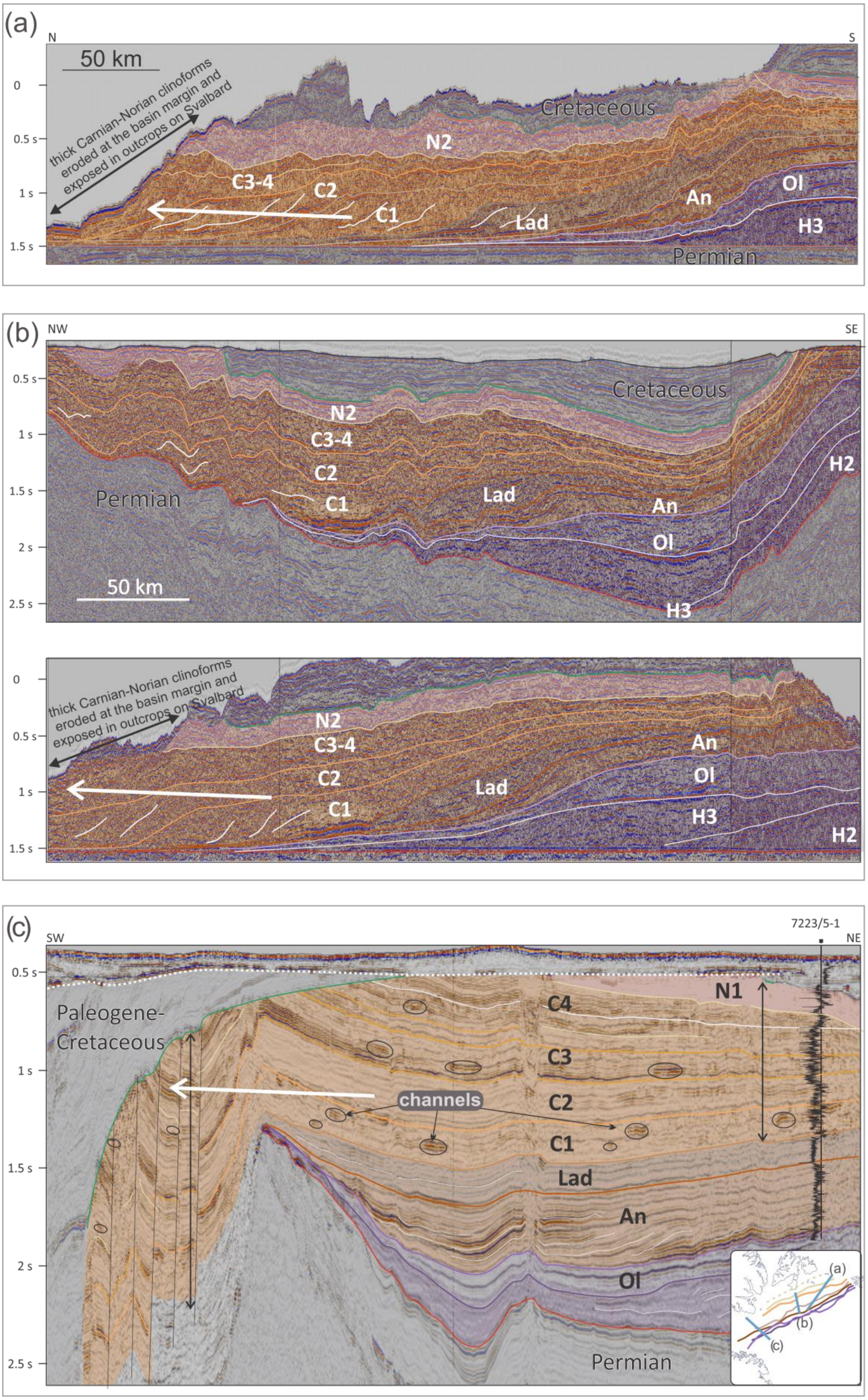

Figure 2: Interpreted regional 2D seismic data, flattened on the base of Triassic, showing the Arctic Barents Sea margin (a), the Barents Sea towards Svalbard margin (b), and the Atlantic Barents Sea margin (c), with a location map of the W Barents Sea showing the line locations. For all these lines, note in particular the large progradational distance of the Carnian section, and that the Carnian is thick but truncated by modern erosion at the margins of the basin, strongly suggesting that the Carnian sedimentary system prograded far beyond the present-day confines of the Greater Barents Sea Basin. Note also the large progradational distance of the Induan and the comparatively small progradational distance of the Olenekian-Ladinian.

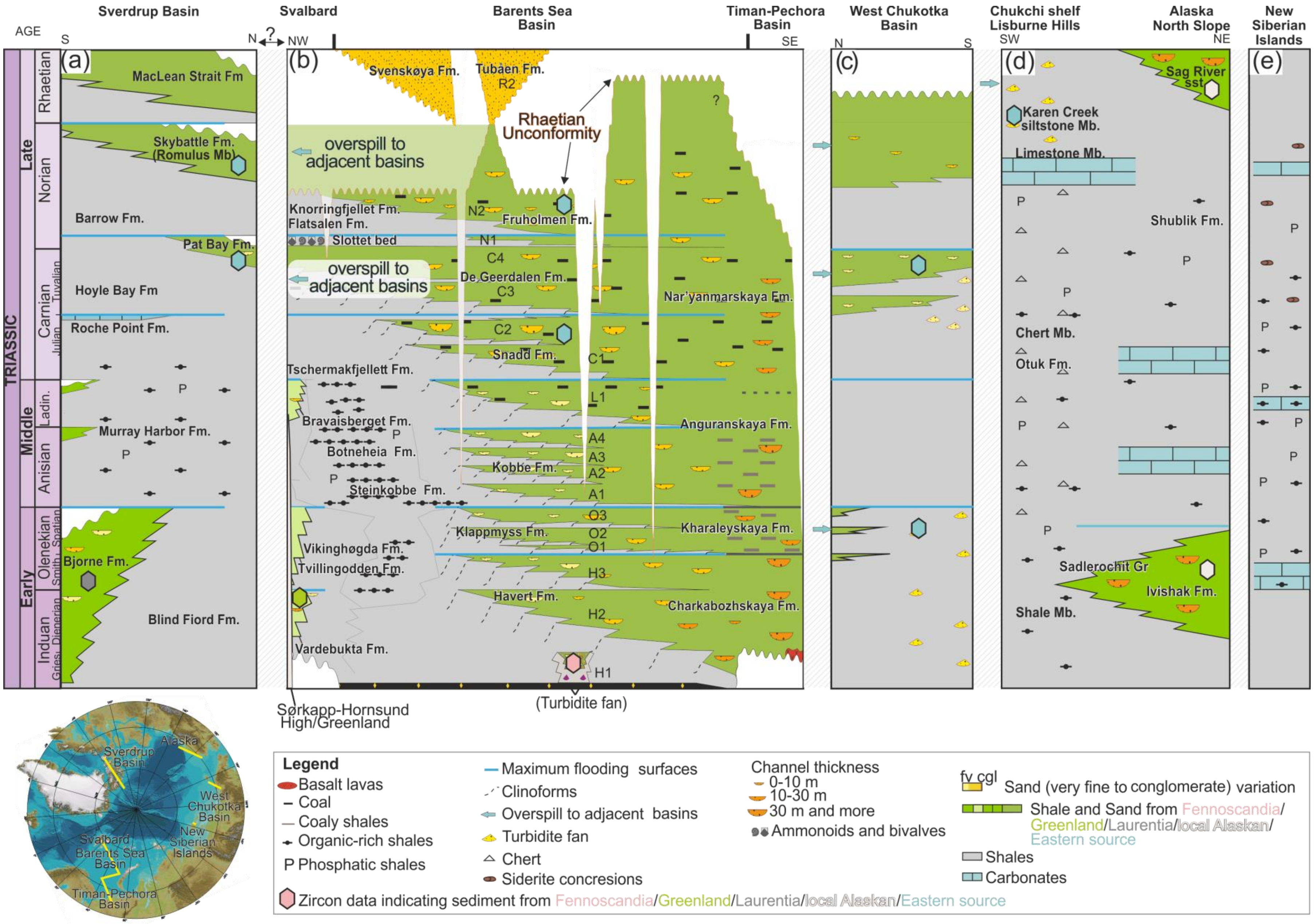

Figure 3: Compiled lithostratigraphic charts and generalized provenance information of the study area and adjacent sedimentary basins, (a) Sverdup Basin (b) Greater Barents Sea Basin, (c) West Chukotka Basin, (d) Chukchi Shelf and Alaskan North Slope, and (e) the New Siberian Islands. Note the influx of mudstone-rich sedimentary deposits with a typical Uralo-Siberian detrital zircon signature in the Early and Late Triassic for West Chukotka, in the Late Triassic for the Sverdup Basin, and for the Carnian on the Chukchi Shelf, indicating a gradual NW-wards progradation of the Uralo-Siberian-sourced sedimentary system in the Late Triassic.

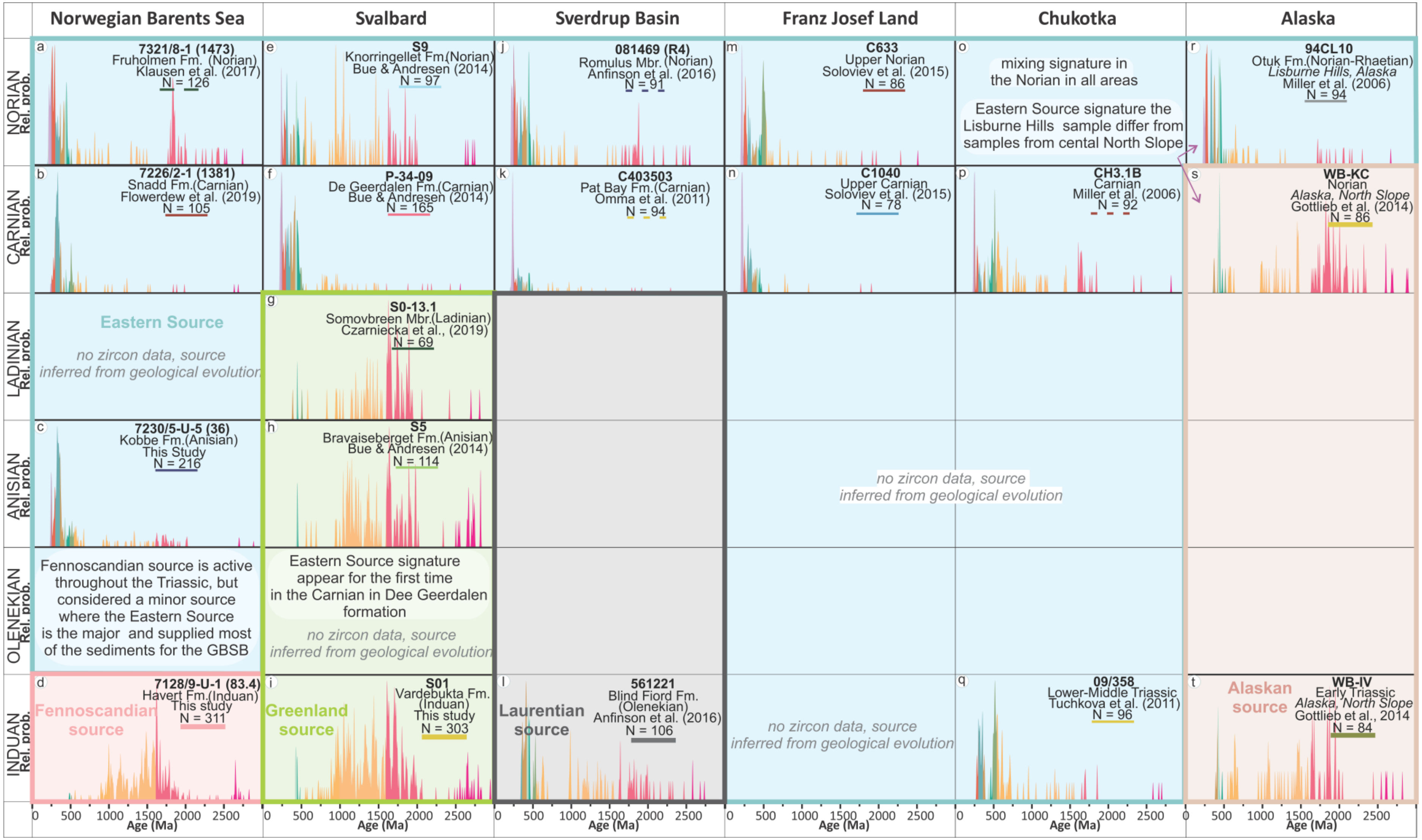

Figure 4: Compiled published and new detrital zircon age-spectra from the sedimentary systems in the Greater Barents Sea Basin and adjacent arctic basins. Note that local detrital zircon signatures (red, green, grey, brown backgrounds) in each of the basin are replaced by the typical Uralo-Siberian signature (blue background) through the Triassic, with replacement happening early in the more proximal areas (GBSB, Chukotka), later in the more distal basins (Svalbard, Sverdrup Basin) and latest in the most distal Alaskan basin. For sample locations, see Fig. 5b.

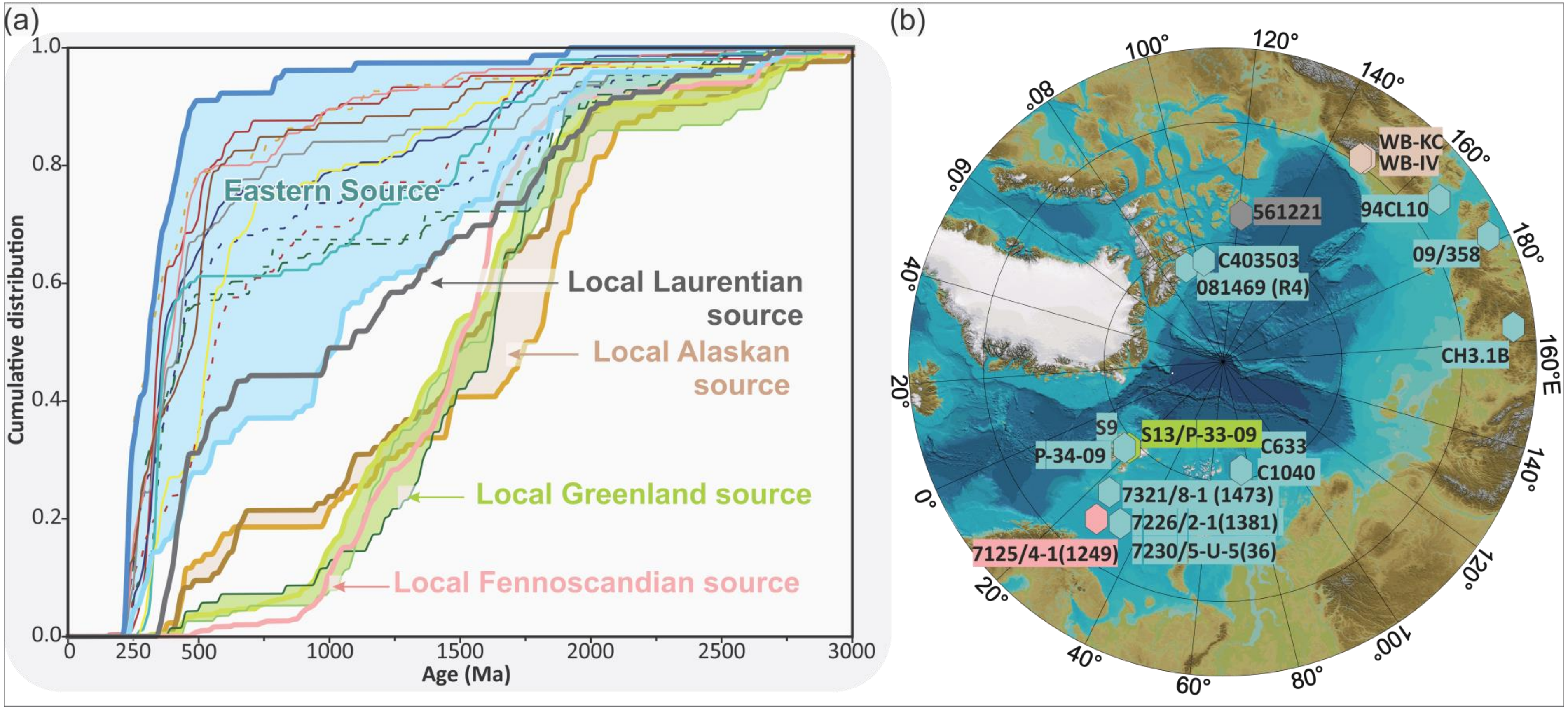

Figure 5: a) Cumulative detrital zircon age spectra for the various samples in Fig. 4, highlighting the difference between the local sources and the Eastern source. Colours are the same as the lines bounding the zircon spectra in Fig. 4. b) Map showing locations of the different samples presented in Figs 4 and 5a.

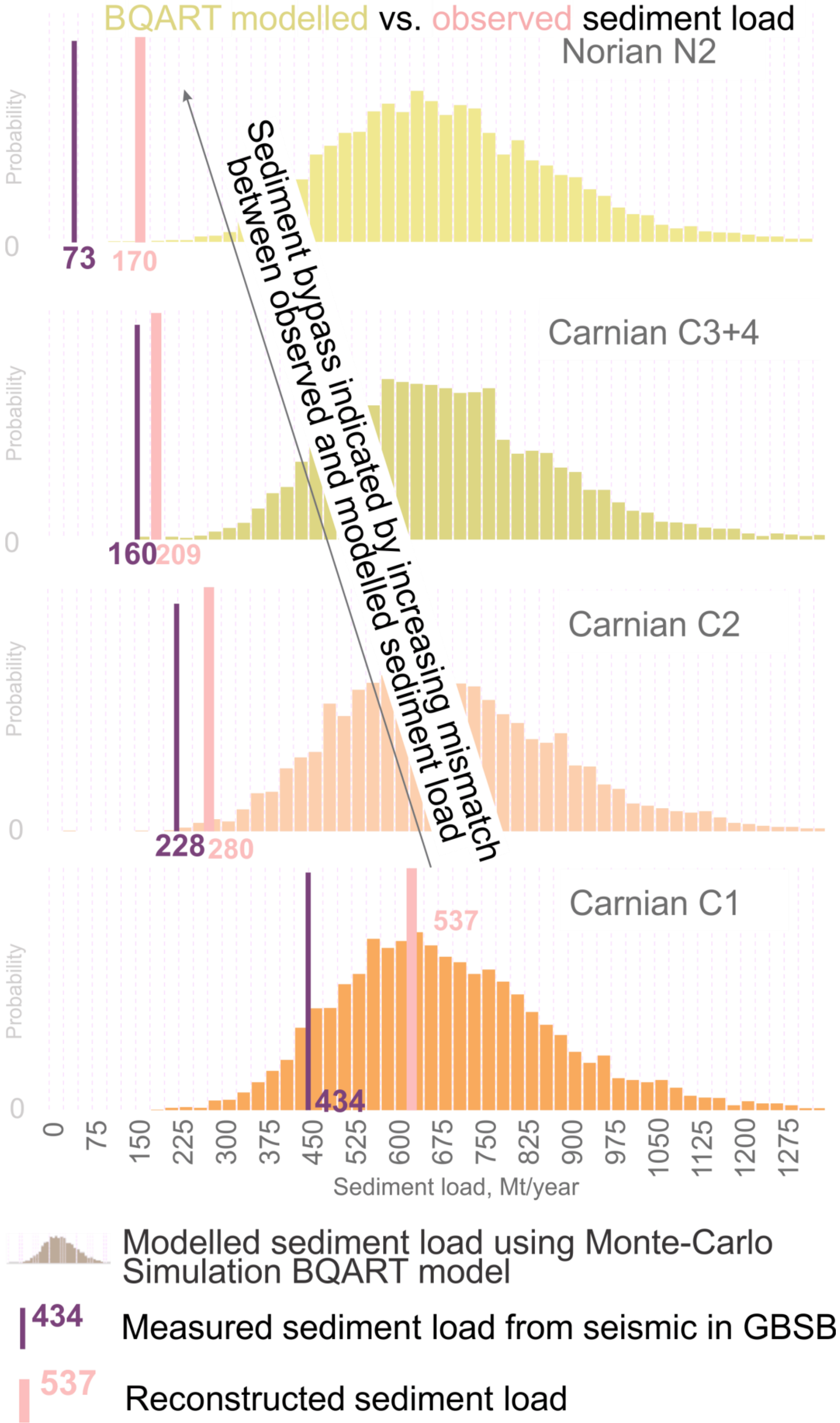

Figure 6: Probability distributions for modelled sediment supply from the Uralo-Siberian sediment source to the GBSB for the investigated Carnian and Norian time periods, and how these models relate to observed (where erosion is not accounted for) and reconstructed (erosion accounted for) sediment supply to the GBSB. Note that for the C1 interval, when the clinoforms did not prograde beyond the GBSB, the modelled and reconstructed sediment supply matches. For the later time steps, there is a progressive mismatch between modelled and observed sediment load, indicating that progressively larger amounts of sediment were bypassed from the GBSB to adjacent basins. Distributions shown are after Gilmullina et al., (2021b).

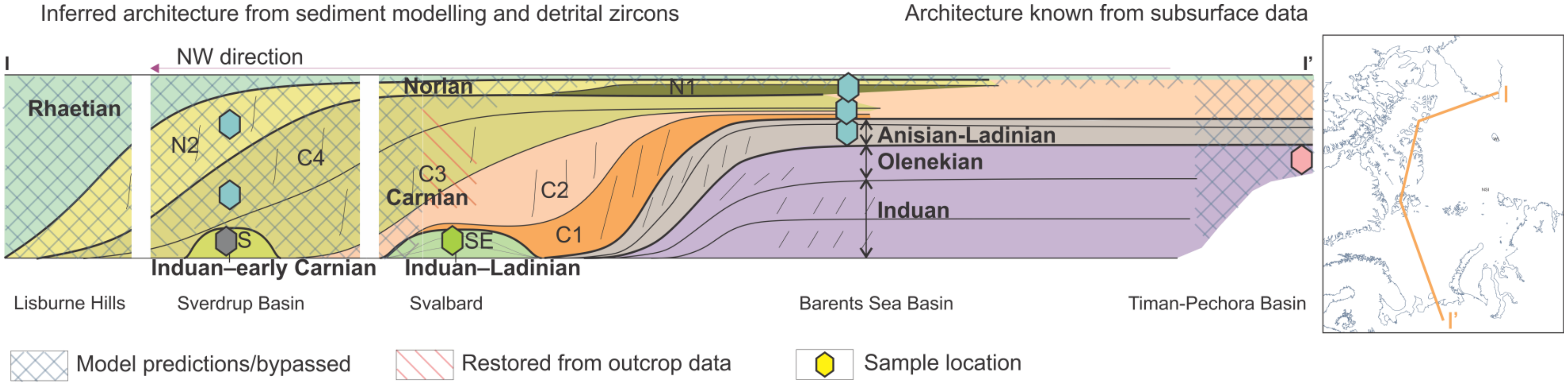

Figure 7: Schematic distribution of sedimentary architecture in the Arctic basins, and the relationship between observed sediments in the GBSB and on Svalbard assumed bypassed sediments to basins beyond.

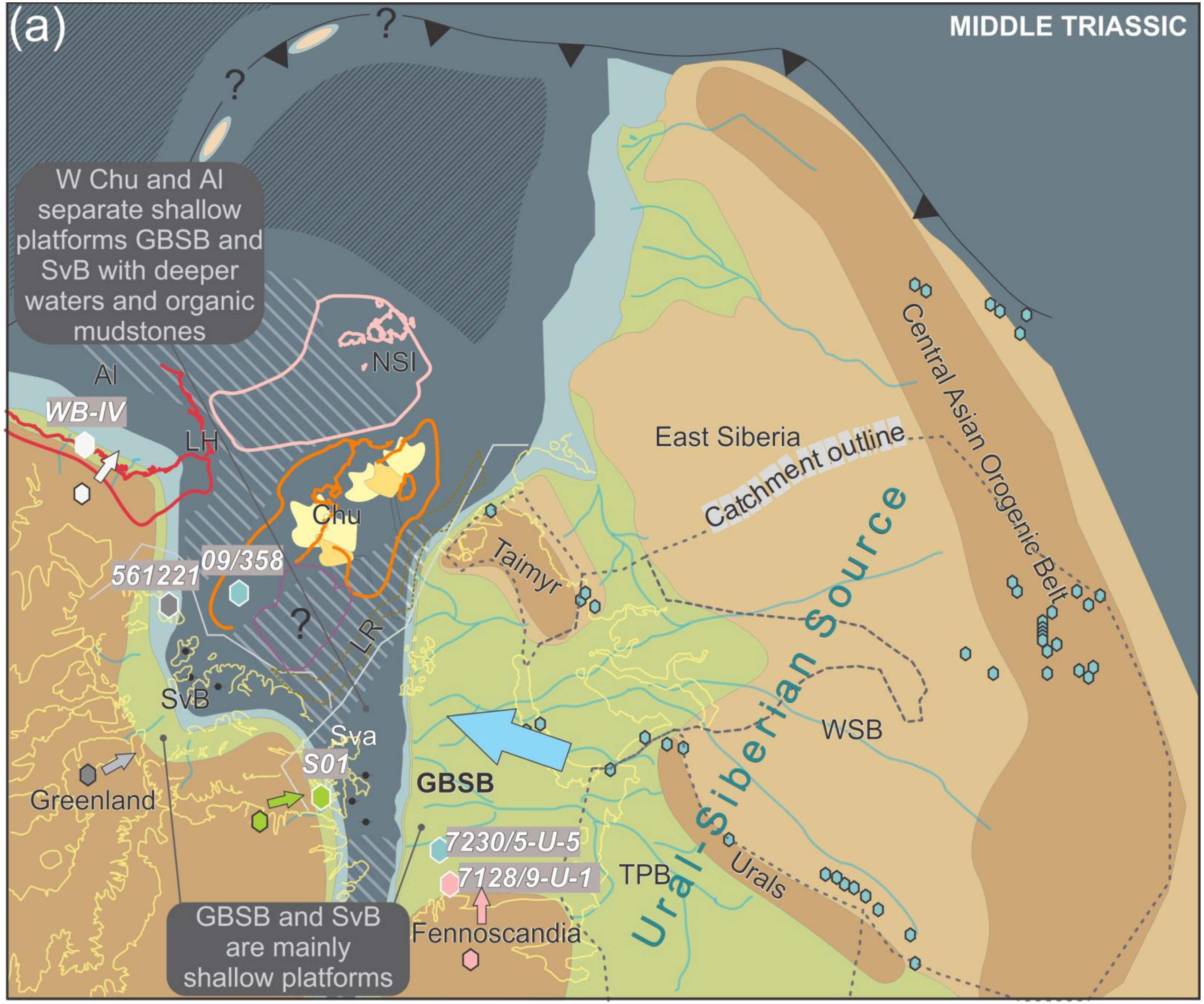

Figure 8: Paleogeographic map of the Arctic and surrounding regions during the Middle Triassic. This time period was characterized by relatively low terrigenous sediment supply and upwelling-related deposition of phosphatic, organic rich mudstones in several of the Arctic basins. For legend, see Figure 11.

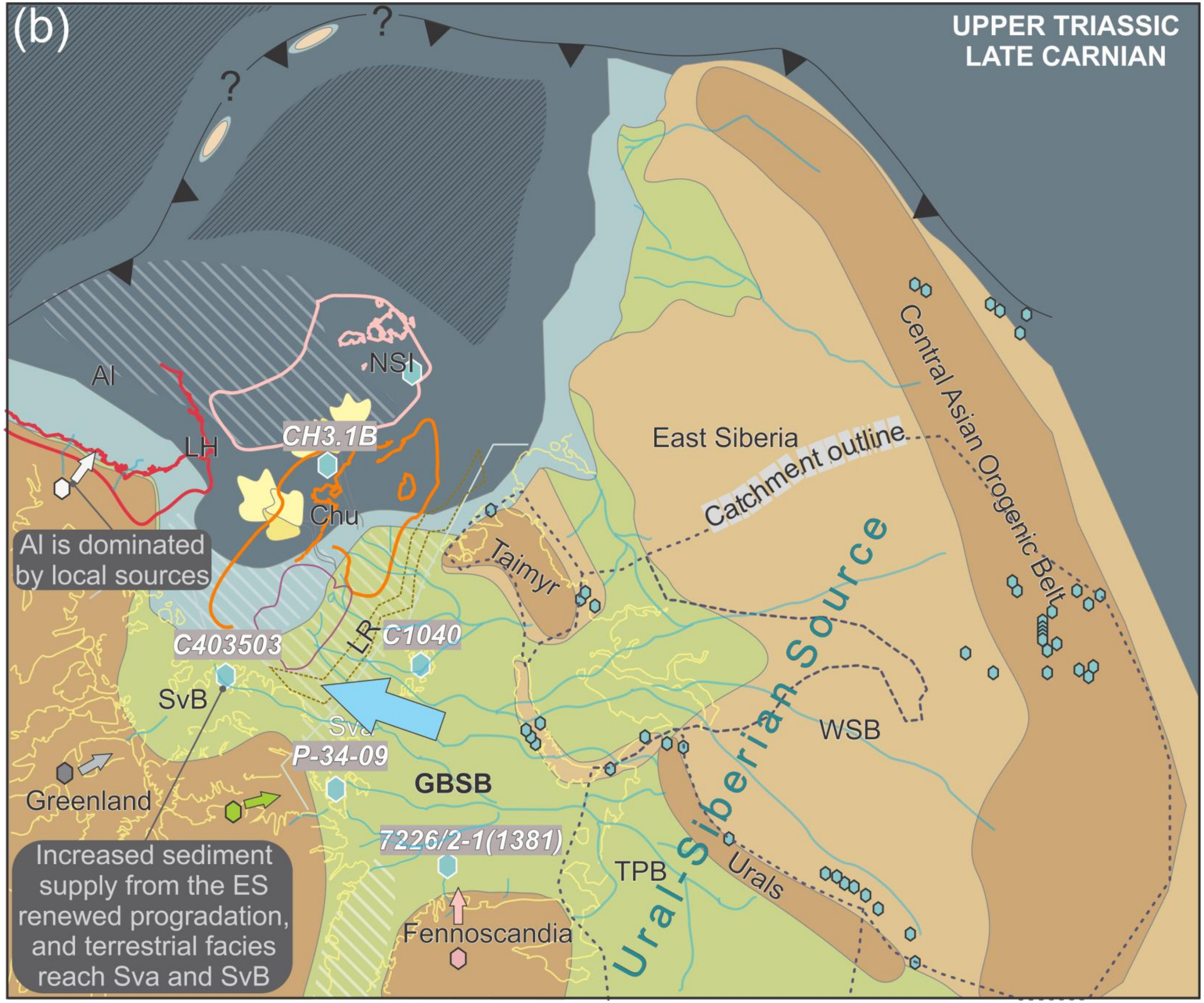

Figure 9: Paleogeographic map of the Arctic and surrounding regions during the Late Triassic Carnian stage. This time period was characterized by very high terrigenous sediment supply from the Polar Urals and incipient uplift of Novaya Zemlya. The progradation of typical Uralo-Siberian sediments into the Sverdrup Basin and progradation from sandy deep marine fans to shallow marine deposits in Chukotka was likely a result of this sediment supply. Alaska is dominated by local sources at this time, indicating that the Uralo-Siberian system did not reach this far. For legend, see Figure 11.

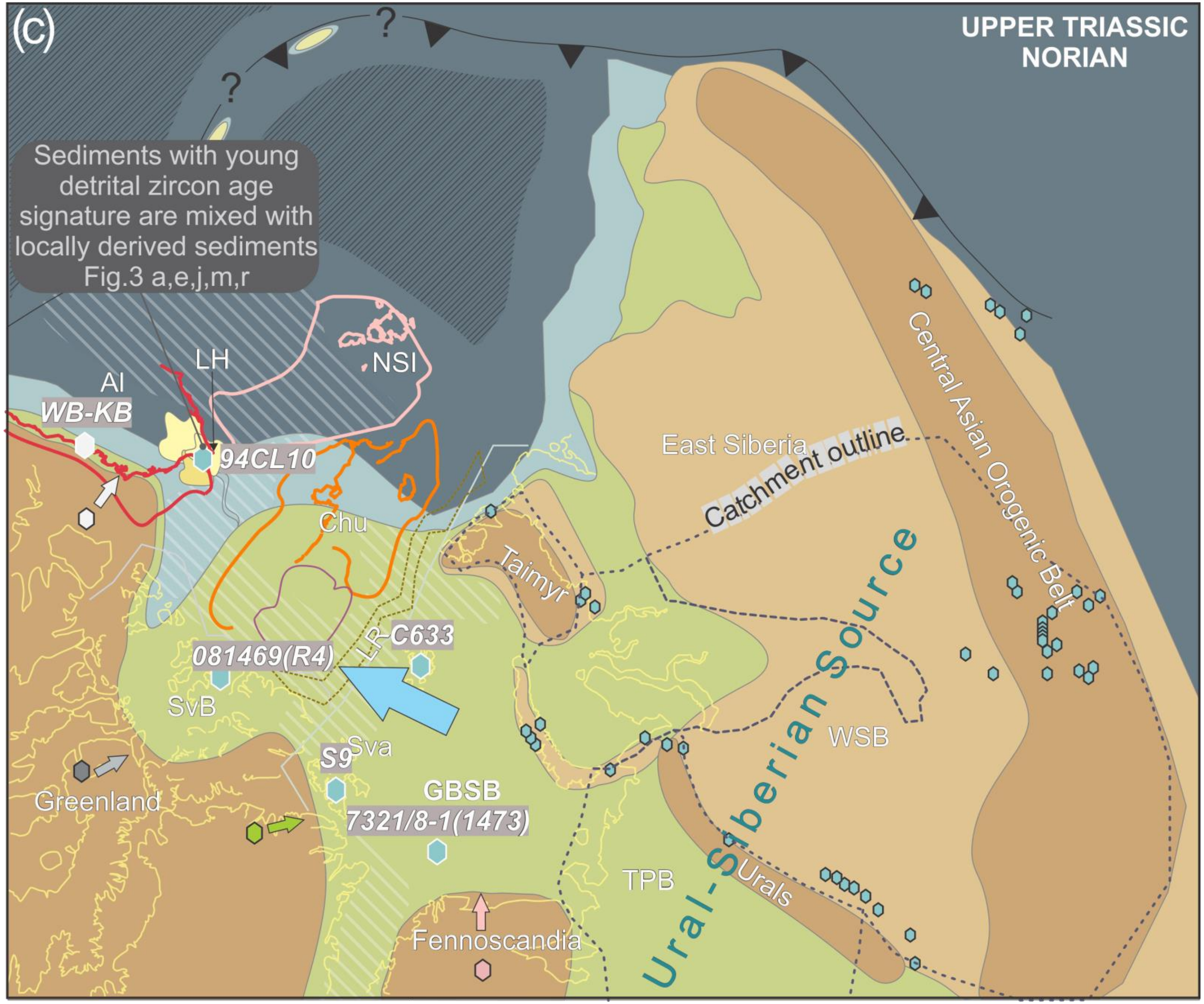

Figure 10: Paleogeographic map of the Arctic and surrounding regions during the Late Triassic Norian stage. This time period was also characterized by very high terrigenous sediment supply from the Polar Urals and incipient uplift of Novaya Zemlya. This time period records the largest extent of terrestrial and shallow-marine sediments with an Uralo-Siberian signature, and turbiditic sandstones in Lisburne Hills show the typical detrital zircon signature during this time. Significant terrigenous deposits have not been recorded on the New Siberian islands. For legend, see Figure 11.

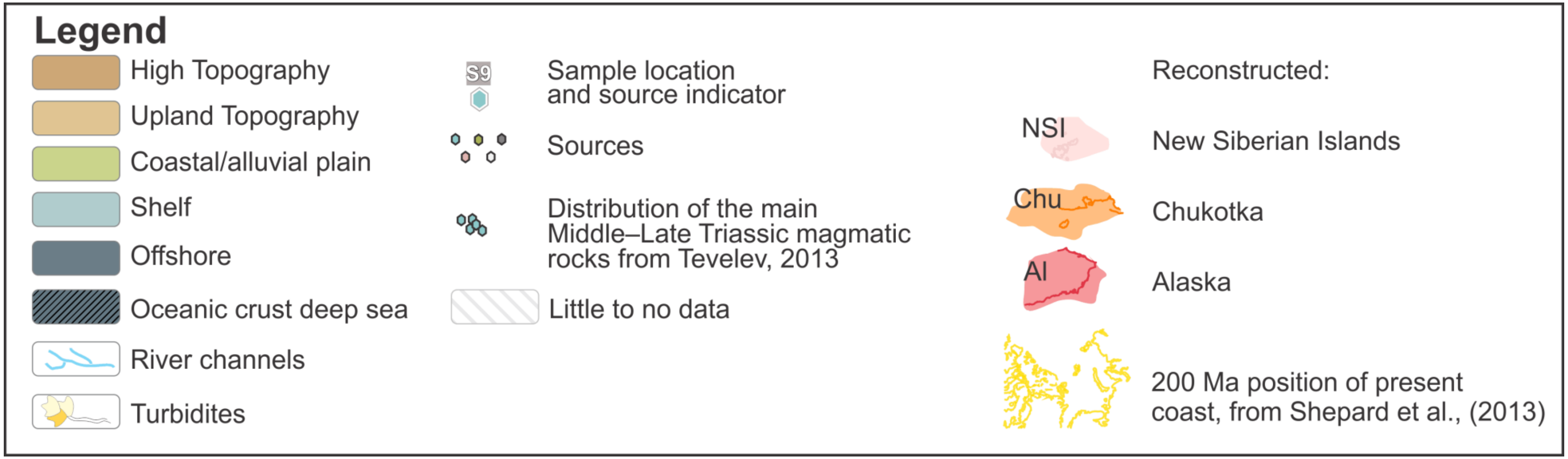

Figure 11: Legend for Figures 8-10.

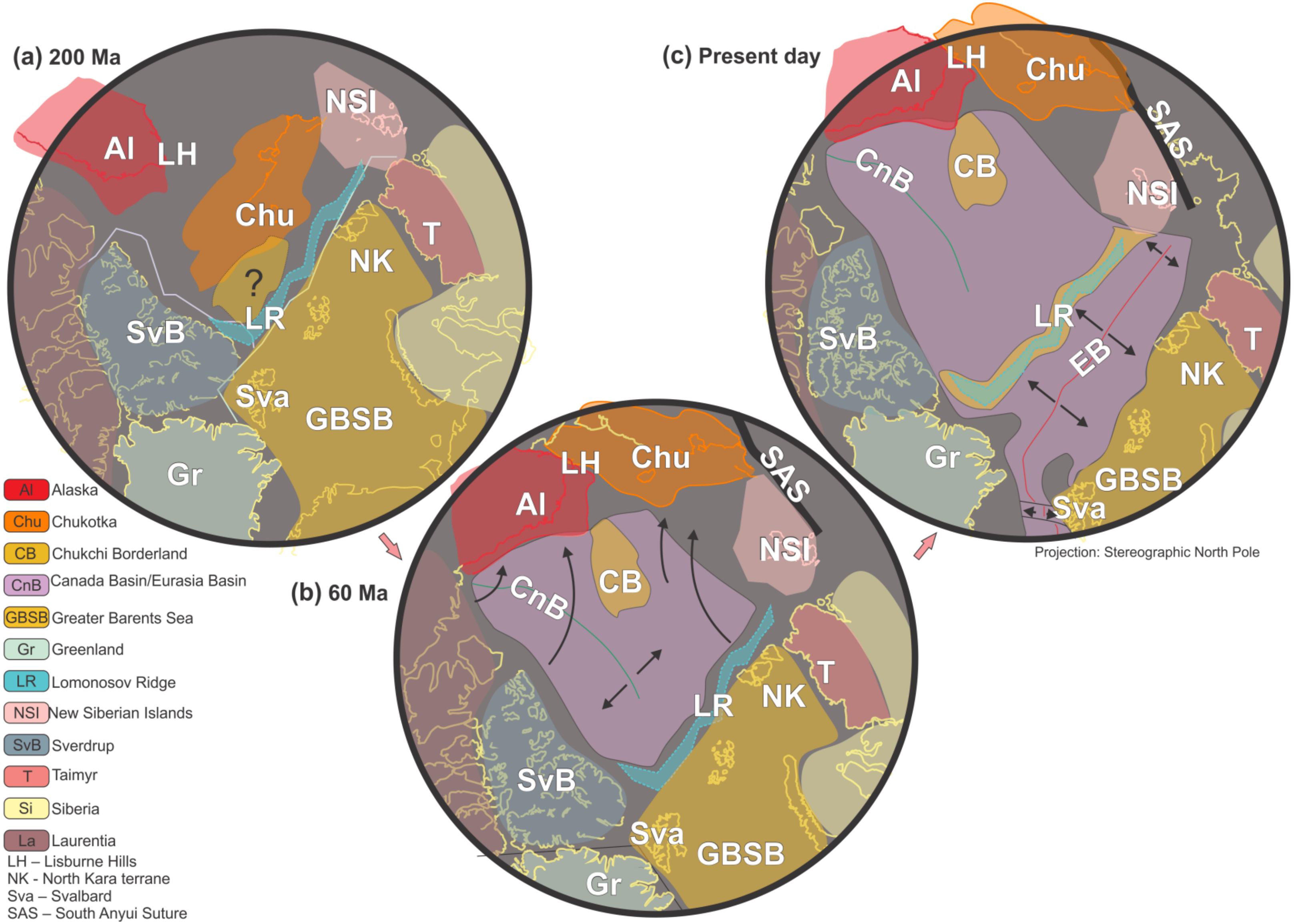

Figure 12: Suggested paleogeographic reconstructions based on the constraints provided by the sedimentary evidence presented herein. a) Most likely pre-breakup setting at the end of the Triassic. The sedimentary evidence requires a distal position of the New Siberian Islands, a close docking of the GBSB, Chukchi Borderland and Chukotka; and a position of the Chukotka Basin and Arctic Alaska near Laurentia; b) Opening of the Amerasia Basin, where Alaska and Chukotka rotate counter-clockwise away from Laurentia; c) Opening of the Eurasia basin, in which the Lomonosov Ridge is rifted off and drifts away from the N margin of the GBSB, with transform motion distancing the previously adjacent Sverdrup Basin and GBSB.